2,2′:6′,2″-Terpyridine (terpy) acting as a Fluxional Bidentate Ligand. Part 2.[1] Rhenium Carbonyl Halide Complexes, *fac*-[ReX(CO)$_3$(terpy)] (X = Cl, Br or I): NMR Studies of their Solution Dynamics, Synthesis of *cis*-[ReBr(CO)$_2$(terpy)] and the Crystal Structure of [ReBr(CO)$_3$(terpy)]†

Edward W. Abel,[a] Valentin S. Dimitrov,[b] Nicholas J. Long,[a] Keith G. Orrell,*[a] Anthony G. Osborne,[a] Helen M. Pain,[a] Vladimir Šik,[a] Michael B. Hursthouse[c] and Mohammed A. Mazid[c]

[a] *Department of Chemistry, The University, Exeter EX4 4QD, UK*
[b] *Institute of Organic Chemistry, Bulgarian Academy of Sciences, Sofia 1113, Bulgaria*
[c] *School of Chemistry and Applied Chemistry, University of Wales, College of Cardiff, Cardiff CF1 3TB, UK*

Under mild conditions pentacarbonylhalogenorhenium(I) complexes react with 2,2′:6′,2″-terpyridine (terpy) to form stable octahedral tricarbonyl complexes *fac*-[ReX(CO)$_3$(terpy)] (X = Cl, Br or I) in which the terpyridine acts as a bidentate chelate ligand. Under more severe reaction conditions *fac*-[ReBr(CO)$_3$(terpy)] can be converted to *cis*-[ReBr(CO)$_2$(terpy)]. In solution the tricarbonyl complexes are fluxional with the terpyridine oscillating between equivalent bidentate bonding modes. At low temperatures rotation of the unco-ordinated pyridine ring is restricted and in CD_2Cl_2 solution two preferred rotamers exist in approximately equal abundances. Rotational energy barriers have been estimated for the X = Cl and I complexes. The X-ray crystal structure of *fac*-[ReBr(CO)$_3$(terpy)] confirms the bidentate chelate bonding of terpy with a N–Re–N angle of 74.3°. The pendant pyridine ring is inclined at an angle of 52.9° to the adjacent co-ordinated ring and the unco-ordinated nitrogen is directed towards the axial carbonyl and *trans* to Br.

2,2′:6′,2″-Terpyridine (terpy) has been used as a ligand towards transition metals for over fifty years but more recently there has been an increase in interest in its co-ordination compounds, prompted by the photochemical properties of some of these complexes.[2] In principle terpy should be able to bond to metal ions as a mono-, bi- or ter-dentate ligand, but in practice the majority of terpy complexes involve terdentate bonding. It is well known[3] that the pentacarbonylhalogenorhenium(I) complexes react readily with ligands to displace two carbonyl groups with the formation of stable octahedral complexes of *fac* stereochemistry. Further displacement of carbonyl groups usually requires rather severe conditions. In an effort to widen the range of compounds in which terpy is acting as a bidentate chelate ligand,[4–10] we have investigated its reactions with the pentacarbonyl halides of rhenium(I), in the expectation that compounds containing bidentate, chelating terpy would be readily isolated and with the possibility of converting them to compounds containing a terdentate chelate terpyridyl ligand.

We have recently reported[11] our preliminary results in this area together with related studies on complexes of terpy with Pt^{IV} and W^0, in which it was shown that in solution terpy was definitely acting in a bidentate chelate mode and was also undergoing an oscillatory fluxional motion. The complete results of our study of the reactions of trimethylplatinum halides with terpy have recently been published.[1]

This paper describes the reactions of the rhenium pentacarbonyl halides [ReX(CO)$_5$] (X = Cl, Br or I) with terpy, solution NMR studies of the dynamic stereochemistry of the resulting *fac*-[ReX(CO)$_3$(terpy)] complexes, the conversion of *fac*-[ReBr(CO)$_3$(terpy)] to *cis*-[ReBr(CO)$_2$(terpy)] and the crystal structure of the complex [ReBr(CO)$_3$(terpy)].

† *Supplementary data available:* see Instructions for Authors, *J. Chem. Soc., Dalton Trans.*, 1993, Issue 1, pp. xxiii–xxviii.

Experimental

Materials.—The compounds [ReX(CO)$_5$] (X = Cl, Br or I) were prepared by previous methods.[12,13] 2,2′:6′,2″-Terpyridine (terpy) was purchased from Aldrich.

Synthesis of Complexes.—All preparations were carried out using standard Schlenk techniques[14] under purified nitrogen using freshly distilled, dried and degassed solvents.

The complexes [ReX(CO)$_3$(terpy)] (X = Cl, Br or I) were all prepared in a similar manner. The details for [ReBr(CO)$_3$(terpy)] are given below. The synthetic and analytical data for the three complexes are given in Table 1.

Bromotricarbonyl(2,2′:6′,2″-terpyridyl)rhenium(I).—The complex [ReBr(CO)$_5$] (0.3 g, 0.74 mmol) and terpyridine (0.18 g, 0.77 mmol) were dissolved in benzene (15 cm^3) with gentle warming to produce a colourless solution. Light petroleum (b.p. 80–100 °C, 15 cm^3) was added and the mixture heated under reflux for 4 h. The product precipitated as a yellow solid. The benzene was removed under reduced pressure and the virtually colourless petroleum decanted. The solid was washed with light petroleum (b.p. 40–60 °C, 25 cm^3) and then dried under vacuum. Recrystallisation from chloroform gave the desired product as bright yellow crystals. Yield 0.42 g (97%).

Bromodicarbonyl(2,2′:6′,2″-terpyridyl)rhenium(I). The com-

Table 1 Synthetic and analytical data for the complexes [ReX(CO)$_3$(terpy)] (X = Cl, Br or I)

Complex	Reaction time/h	M.p.[a]/°C	Yield[b] (%)	ν_{CO}[c]/cm^{-1}	Analysis[c] (%) C	H	N
[ReCl(CO)$_3$(terpy)]	3.5	267–269	84	2026vs, 1922s, 1898s	40.1 (39.6)	2.1 (2.3)	7.8 (7.7)
[ReBr(CO)$_3$(terpy)]	3	278–280	97	2030vs, 1930s, 1900s	37.1 (37.3)	1.9 (1.8)	7.2 (7.1)
[ReI(CO)$_3$(terpy)]	4	263–265	77	2026vs, 1928s, 1920s	34.3 (34.6)	1.7 (1.8)	6.7 (6.6)

[a] With decomposition. [b] Yield quoted relative to [ReX(CO)$_5$]. [c] Recorded in CH_2Cl_2 solution; s = strong, v = very. [d] Calculated values in parentheses.

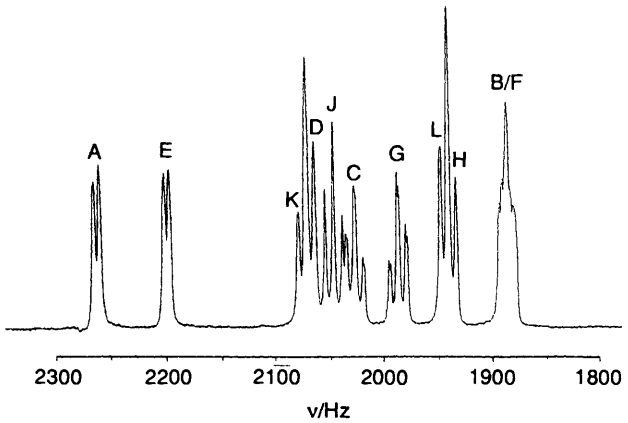

Fig. 1 250 MHz ^{1}H NMR spectrum of [ReBr(CO)$_3$(terpy)] in $CDCl_2CDCl_2$ at −10 °C. Signal labels refer to Fig. 2

plex [ReBr(CO)$_3$(terpy)] (0.2 g, 0.34 mmol) was sealed in an evacuated glass Carius tube and placed in an oven at 270 °C for 5 h. After cooling, the dark brown solid was removed from the tube, washed with chloroform (3 × 10 cm^3) and dried *in vacuo*. Yield 0.19 g (100%) (Found: C, 36.8; H, 2.0; N, 7.1. $C_{17}H_{11}BrN_3O_2Re$ required C, 36.8; H, 2.0; N, 7.6%). IR [Me_2SO]: 1889s and 1817s cm^{-1}.

Physical Methods.—Hydrogen-1 NMR spectra were recorded on a Bruker AM250 spectrometer operating at 250.13 MHz. All spectra were recorded in CD_2Cl_2 or $CDCl_2CDCl_2$ solutions with $SiMe_4$ as the internal standard. A standard B-VT1000 variable-temperature unit was used to control the probe temperature, the calibration of this unit being checked periodically against a Comark digital thermometer. The temperatures are considered accurate to ±1 °C. Rate data were based on band-shape analysis of ^{1}H spectra using the authors' version of the standard DNMR program.[15] Activation parameters based on experimental rate data were calculated using the THERMO program.[16] Infrared spectra were recorded on a Perkin Elmer 881 spectrometer, calibrated from the 1602 cm^{-1} signal of polystyrene. Elemental analyses were performed by Butterworth Laboratories Ltd., Teddington, Middlesex, London.

X-Ray Structural Determination of [ReBr(CO)$_3$(terpy)].—*Crystal data.* $C_{18}H_{11}BrN_3O_3Re$, M = 583.42, monoclinic, space group C_2/c, a = 26.902(3), b = 8.790(1), c = 15.228(2) Å, β = 95.19(1)°, U = 3586.18 Å^3, Z = 8, D_c = 2.16 g cm^{-3}, $F(000)$ = 2192, Mo-Kα radiation (λ = 0.710 69 Å), μ = 90.98 cm^{-1}.

Data collection and processing. Data were collected using a FAST TV area detector diffractometer situated at the window of a rotating anode generator operating at 50 kV, 55 mA with a molybdenum anode, as described previously.[17] Somewhat more than one hemisphere of data was recorded for which 9801 reflections were measured, giving 2587 unique and 2231 observed with $F_o > 3\sigma(F_o)$.

Structural analysis and refinement. The structure was solved by standard Patterson methods. Full-matrix least squares were performed with non-hydrogen atoms assigned anisotropic thermal parameters. Hydrogen atoms were allowed to ride on their parent carbon atoms in the calculated positions (C–H 0.96 Å). The final R and R' (unit weights) were 0.036 and 0.042 respectively for the 238 variables. The computer programs used are given in ref. 18.

Additional material available from the Cambridge Crystallographic Data Centre comprises H-atom coordinates, thermal parameters and remaining bond lengths and angles.

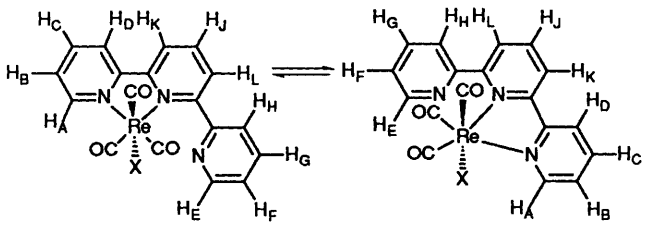

Fig. 2 Interconverting structures of [ReX(CO)$_3$(terpy)] complexes showing the hydrogen labelling

Results and Discussion

Excellent yields of the complexes [ReX(CO)$_3$(terpy)] (X = Cl, Br or I) as air-stable, yellow crystalline solids were obtained following the above method. In solution the complexes showed three strong carbonyl stretching bands (Table 1) which is indicative of a *fac* stereochemistry for the complexes, and hence for terpy acting as a bidentate chelate ligand. NMR spectroscopy and X-ray crystallography (see below) provided confirmation of this conclusion. Heating a sample of [ReBr(CO)$_3$(terpy)] in a sealed evacuated glass Carius tube produced a dark brown solid which was only sparingly soluble in organic solvents. This compound was identified as *cis*-[ReBr(CO)$_2$(terpy)] on the basis of analytical data, IR data (two carbonyl bands occurring at much lower wavenumbers than for the tricarbonyl species), and the much simpler ^{1}H NMR spectrum which comprised only six chemically shifted signals (Table 2) and is indicative of a terdentate terpyridyl ligand.

Ambient- and Above-ambient-temperature NMR Studies.—[ReX(CO)$_3$(terpy)]. At ambient temperature the ^{1}H NMR spectra of these compounds showed a slight line broadening of all signals with the exception of one triplet. On cooling the solutions to *ca.* −10 °C the spectral lines sharpened and well resolved spectra were obtained. The results from [ReBr(CO)$_3$(terpy)] will demonstrate the analysis of the problem. The spectrum at 263 K (Fig. 1) consisted of multiplets arising from eleven non-equivalent protons of the terpy ligand and hence was clearly associated with the terpy acting in a bidentate chelate mode of bonding to rhenium (Fig. 2). Careful analysis of the

Table 2 Proton NMR chemical shift data* for terpy and its rhenium(I) complexes

Compound	Solvent	T/°C	δ_{AE}	δ_{BF}	δ_{CG}	δ_{DH}	δ_{J}	δ_{KL}
terpy	CD_2Cl_2	30	8.69	7.35	7.88	8.64	7.96	8.47
[ReBr(CO)$_2$(terpy)]	$(CD_3)_2SO$	30	8.90	7.48	8.04	8.56	8.22	8.60
[ReBr(CO)$_3$(terpy)]	$(CDCl_2)_2$	140	8.99	7.50	8.03	8.08	8.12	8.01
[ReBr(CO)$_3$(terpy)]	$(CDCl_2)_2$	−10	9.05 (A)	7.55 (B)	8.11 (C)	8.27 (D)	8.18	8.29 (K)
			8.80 (E)	7.54 (F)	7.94 (G)	7.74 (H)		7.77 (L)
[ReCl(CO)$_3$(terpy)]	$(CDCl_2)_2$	0	9.03 (A)	7.54 (B)	8.12 (C)	8.25 (D)	8.18	8.28 (K)
			8.80 (E)	7.54 (F)	7.95 (G)	7.77 (H)		7.77 (L)
[ReI(CO)$_3$(terpy)]	$(CDCl_2)_2$	0	9.09 (A)	7.54 (B)	8.08 (C)	8.26 (D)	8.17	8.29 (K)
			8.80 (E)	7.51 (F)	7.94 (G)	7.73 (H)		7.73 (L)

* Relative to $SiMe_4$ (internal), $\delta = 0$. See Fig. 2 for hydrogen labelling.

Table 3 Proton NMR scalar coupling constant data[a] for terpy and its rhenium(I) complexes

Compound	J_{AB}/J_{EF}	J_{AC}/J_{EG}	J_{AD}/J_{EH}	J_{BC}/J_{FG}	J_{BD}/J_{FH}	J_{CD}/J_{GH}	J_{JK}/J_{JL}
terpy	4.8	1.8	0.8	7.5	1.2	8.0	7.9
[ReBr(CO)$_2$(terpy)]	5.5	1.5	0.7	7.7	1.3	8.2	8.1
[ReBr(CO)$_3$(terpy)]	4.8/4.8	1.8/1.8	*b*	7.5/7.5	*b*	8.0/8.0	7.9/7.9
[ReCl(CO)$_3$(terpy)]	5.0/4.5	*b*	*b*	7.1[c]/7.1[c]	*b*	7.4/7.4	8.0/7.5
[ReI(CO)$_3$(terpy)]	5.2/4.1	*b*	*b*	6.8[c]/5.7[c]	*b*	7.9/7.7	7.3/7.7

[a] In Hz. See Fig. 2 for hydrogen labelling of [ReX(CO)$_3$(terpy)] species. [b] Not measured accurately. [c] Values less accurate due to small $\delta_B - \delta_F$ value.

spectrum involving proton-decoupling experiments established the unambiguous assignment of all eleven protons, labelled A–K in Figs. 1 and 2. All chemical shifts and coupling constant data are given in Tables 2 and 3. The pseudo-triplets attributable to the proton pairs D/K and H/L were overlapping 1:1 doublets and the lowest frequency multiplet, for B/F, arose from two closely overlapping triplets. Hydrogens H_A and H_E, α to the N atoms, give rise to the signals at highest frequency, with H_A experiencing an additional co-ordination induced shift.

On increasing the solution temperature, extensive changes occurred in the ^{1}H NMR spectrum as indicated in Fig. 3. Exchange broadening occurred between analogous pairs of protons in the outer rings, namely, $H_{A/E}$, $H_{B/F}$, $H_{C/G}$ and $H_{D/H}$ according to the spin problem ABCD $\rightleftharpoons$ EFGH, and also between protons H_K and H_L of the central ring, according to the spin problem JKL $\rightleftharpoons$ JLK. The signal due to H_J retained its sharp triplet structure throughout the full temperature range. At 140 °C the exchanges had become rapid on the ^{1}H NMR shift time-scale and a simplified spectrum resulted with only six chemical shifts, three of them due to the proton pairs C/G, D/H, K/L having very similar magnitudes (Table 2).

The observed spectral changes clearly point to the terpyridyl being involved in a fluxional process in which the co-ordination complex is oscillating between two equivalent forms both involving bidentate chelate bonding for terpyridyl (Fig. 2). The energetics of this process were analysed by the application of standard band-shape analysis methods in two separate experiments. First the method was applied to the exchanging pairs of signals A and E and fitting the AE portion of the AB $\rightleftharpoons$ EF dynamic spectrum, then secondly, the whole spectrum *i.e.* ABCD $\rightleftharpoons$ EFGH and JKL $\rightleftharpoons$ JLK was fitted. The experimental and computed spectra are compared in Fig. 3. Considering that the fittings involved eleven chemical shifts and numerous scalar coupling constants the matchings of theoretical and experimental spectra are extremely close and provide an impressive example of the power of total NMR band-shape analysis for extracting rate data. The calculated activation energies for the two separate experiments were identical within experimental error, and for the above reasons are considered to be of high accuracy.

Analogous spectral changes were observed for the other two complexes [ReX(CO)$_3$(terpy)] (X = Cl or I) but in view of the excellent agreement obtained in the two band-shape fitting experiments with the bromide complex band-shape analyses for the chloride and iodide complexes were restricted to the exchanging pairs of signals A/E and B/F.

cis-[ReBr(CO)$_2$(terpy)]. This terdentate terpy complex was stereochemically rigid in solution as expected so no dynamic NMR studies could be performed. A comparison of its room-temperature ^{1}H NMR spectrum with the spectrum of free terpy and the spectra of static and rapidly fluxional [ReBr(CO)$_3$-(terpy)] does, however, provide interesting insight into the different electronic influences of the aromatic terpy protons for non-co-ordinative, bi- and ter-dentate co-ordinative modes of the ligand.

Examination of Table 2 shows that when the free terpy ligand forms a terdentate complex with ReBr(CO)$_2$, hydrogens A/E, B/F, C/G, J and K/L all experience high frequency shifts (Δδ) ranging in magnitude from 0.13 (K/L) to 0.26 (J) ppm. The notable exceptions are the D/H hydrogens where a small low frequency shift (Δδ = 0.08) occurs. In the free ligand the D/H chemical shift appears at a relatively high frequency, presumably the result of deshielding by the central N atom arising from the preferred *trans* orientation of adjacent pyridine rings in free terpy. On complexation, the necessary *cis* orientation of these rings causes a somewhat greater relative shielding effect than the deshielding associated with metal co-ordination. Hence, a small net shielding effect ensues. The same argument can be applied to the K/L hydrogens, but here the deshielding due to the co-ordination slightly outweighs the shielding arising from the 180° switches of the unco-ordinated pyridine ring.

A comparison of the chemical shifts for the complexes [ReBr(CO)$_2$(terpy)] and [ReBr(CO)$_3$(terpy)] reveals significant low frequency shifts of the D/H and K/L hydrogens (Δδ = 0.48 and 0.59 respectively) on going from the terdentate to the bidentate terpy complex. In the terdentate case the D/K and H/L pairs of hydrogens reside in deshielding zones of two pyridine rings. By contrast, in the bidentate species only the D/K pair of hydrogens is so affected, the H/L pair resonating at significantly higher frequencies as a result of the rotation of the pendant pyridine ring which will cause the H/L hydrogens to pass through aromatic shielding zones. The high-temperature, fluxionally averaged shifts for D/H and K/L hydrogen pairs of the bidentate complex will therefore occur at appreciably lower frequencies than for the terdentate complex.

The effect of co-ordination on the scalar H–H couplings in terpy is quite slight (Table 3), the most notable changes being an

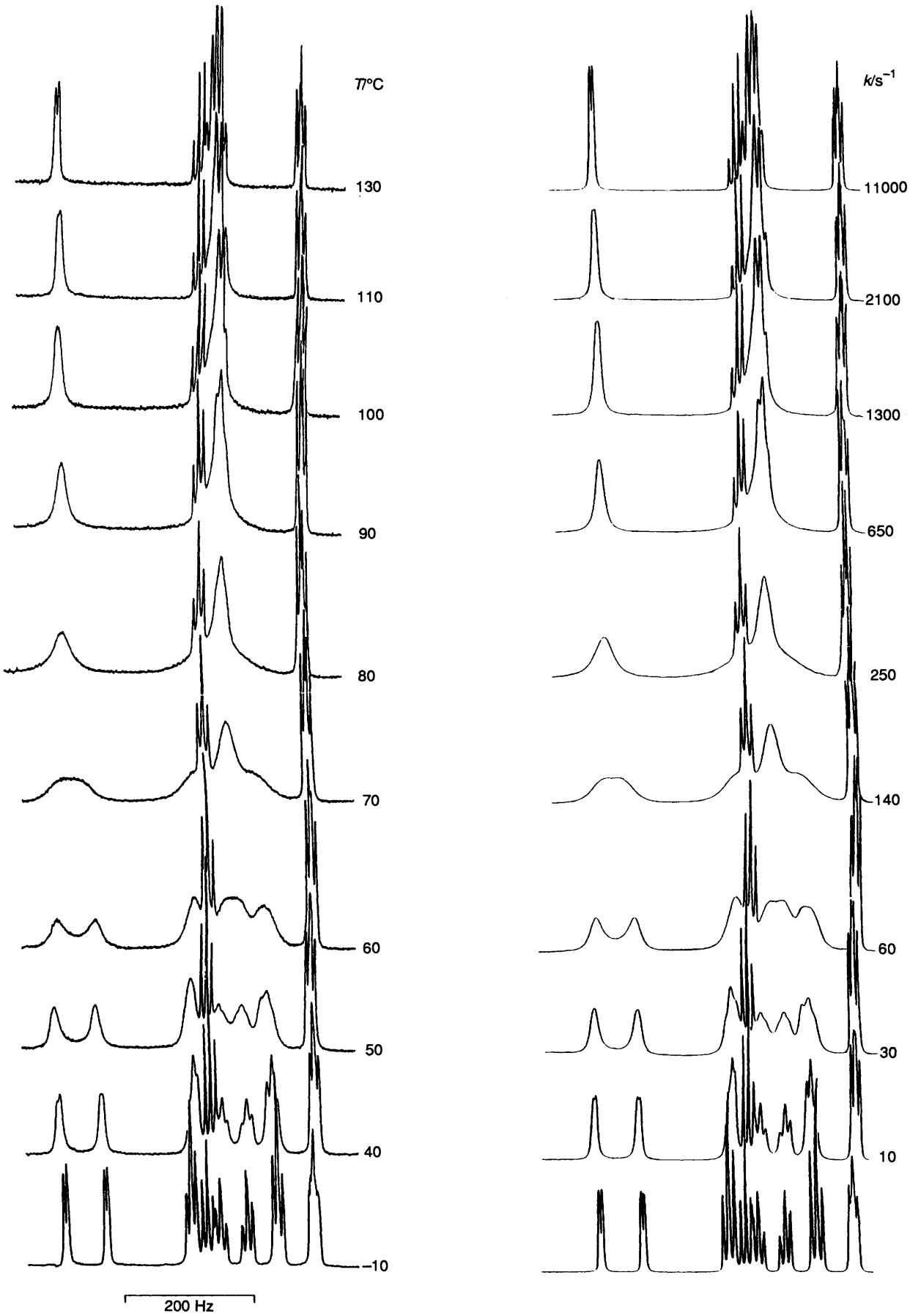

Fig. 3 250 MHz ^{1}H NMR spectra of [$ReBr(CO)_3(terpy)$] in $CDCl_2CDCl_2$ in the temperature range −10 to 130 °C. Computer simulated spectra are shown on the right with 'best-fit' rate constants for the fluxional process

Table 4 Activation parameters for Re–N fluxion in $[ReX(CO)_3(terpy)]$ complexes

X	Temperature range/°C	$\Delta H^{\ddagger}$/kJ mol^{-1}	$\Delta S^{\ddagger}$/J K^{-1} mol^{-1}	$\Delta G^{\ddagger}$[a]/kJ mol^{-1}
Cl	0–140	77.2 ± 1.4	23.2 ± 4.0	70.3 ± 0.2[b]
Br	−10 to 140	79.8 ± 1.7	27.5 ± 4.8	71.6 ± 0.3[c]
I	0–140	76.3 ± 0.9	11.1 ± 2.4	73.0 ± 0.1[b]

[a] At 298.15 K. [b] Value based on band-shape analysis of the exchanging signals AB ⇌ EF. [c] Value based on band-shape analysis of the exchanging signals ABCD ⇌ EFGH and JKL ⇌ JLK.

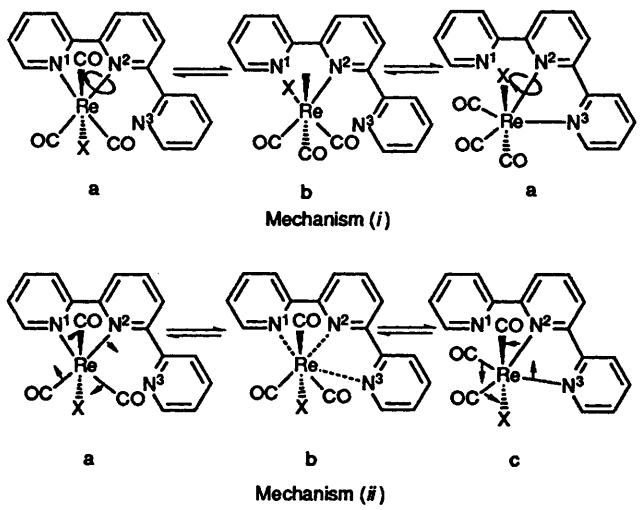

Fig. 4 Two possible mechanisms for the Re–N linkage fluxion, namely the rotation mechanism (*i*) and the 'tick-tock' twist mechanism (*ii*)

increase of J_{AB} ($=J_{EF}$) from 4.8 to 5.5 Hz on formation of the terdentate rhenium(I) complex.

Energies and Mechanism of the Fluxion in $[ReX(CO)_3(terpy)]$ *Complexes.*—Activation parameters for the fluxional process were calculated for 'best-fit' rate data and are listed in Table 4. $\Delta G^{\ddagger}$ Values for the fluxion are in the range 70.3 to 73.0 kJ mol^{-1} and exhibit slight halogen dependence. The only values available for comparison are those from our work with the complexes $[PtXMe_3(terpy)]$ (X = Cl, Br or I) where the $\Delta G^{\ddagger}$ values fall in the range 61.5 to 62.5 kJ mol^{-1}.[1] The ordering of $\Delta G^{\ddagger}$ with respect to metal, *i.e.* Re > Pt, for the metal–terpyridine commutation, is consistent with the order found for these two metals in metal–(sulfur ligand) commutational processes.[19]

Two possible mechanisms for the Re–N commutation are illustrated in Fig. 4. Mechanism (*i*) involves loosening of the Re–N(1) bond followed by 180° rotation of the $ReX(CO)_3$ moiety *via* a five-co-ordinate intermediate to produce the original structure. Mechanism (*ii*) involves the loosening of both Re–N bonds followed by a twist of the $ReX(CO)_3$ moiety through an angle equal to the N(1)–Re–N(2) angle *via* a seven-co-ordinate intermediate to produce the enantiomer of the original structure.

Mechanism (*ii*) was shown to operate in the $[PtXMe_3(terpy)]$ complexes since exchange of the equatorial (*trans* N) Pt–Me environments occurred. Unfortunately the limited solubility of the present rhenium complexes in suitable NMR solvents made it impossible to observe whether the ^{13}C equatorial (*trans* N) carbonyl signals of these complexes were similarly affected. However, in view of the isoelectronic nature of the metal moiety and structural similarity of the metal complexes in the two series we believe that mechanism (*ii*) is also operating in these rhenium complexes.

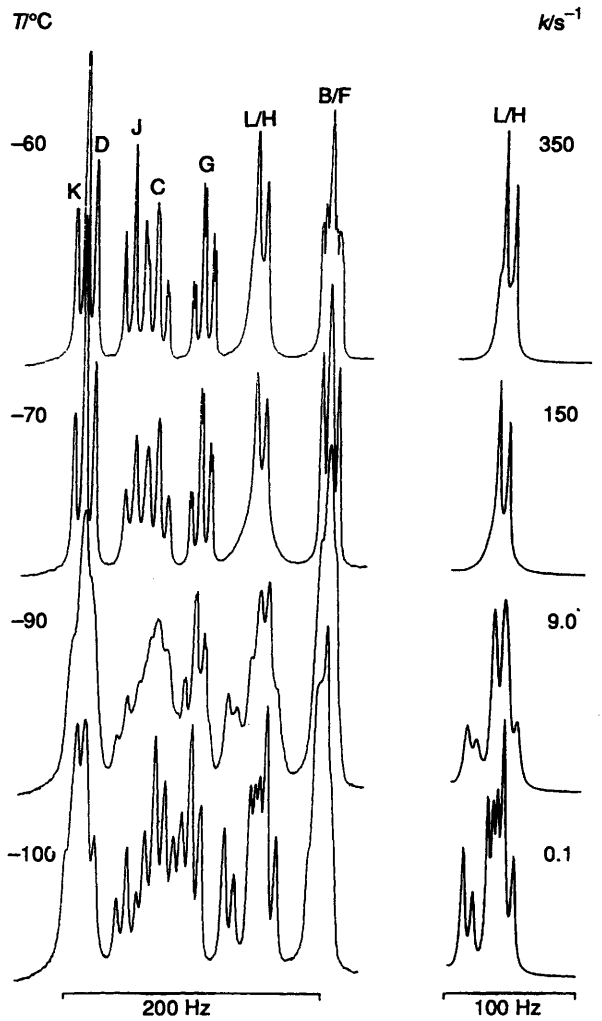

Fig. 5 Low-temperature 250 MHz ^1H NMR spectra of $[ReCl(CO)_3(terpy)]$ in CD_2Cl_2 showing the effects of restricted rotation of the uncoordinated pyridine ring. High frequency signals of hydrogens A and E not shown. Theoretical spectra of the L/H resonance with 'best-fit' rate constants are shown alongside

Low-temperature NMR Studies.—In our previous studies on $[PtXMe_3(terpy)]$,[1] restricted rotation of the pendant, uncoordinated pyridine ring was demonstrated by low-temperature NMR spectra of CD_2Cl_2 solutions of these complexes. The arrest of the pyridine rotation strikingly affects the Pt–Me signals, whilst changes in the aromatic signals are more complex and less easy to interpret. In the present $[ReX(CO)_3(terpy)]$ complexes any restricted rotation effect can, unfortunately, be monitored only by the ^1H aromatic signals, as the ^{13}C carbonyl signals are too weak for any effective study.

On cooling the complexes below *ca.* −50 °C changes occurred in a number of the aromatic hydrogen multiplets as illustrated by $[ReCl(CO)_3(terpy)]$ (Fig. 5). The most significant and informative changes affected the signals of hydrogens H and L, but signals due to C and J were also affected. Attention was given to the changes in the H/L band shape. At temperatures of −50 °C and above this consisted of two overlapping doublets due to three-bond scalar couplings of the hydrogens to their *ortho* neighbours. On cooling, the signals broadened, coalesced and finally at −100 °C split into a well separated pair of doublets ($\Delta\delta$ = 0.12) assigned to the H hydrogens and a closely separated pair of doublets ($\Delta\delta$ = 0.03, only three lines visible) due to the L hydrogens. These pairs of signals clearly represent two different rotameric forms of the complex due to the 'freezing' of the pendant pyridine rotation. The 'static' spectrum at −100 °C was simulated as shown in Fig. 5. The 'best-fit' was

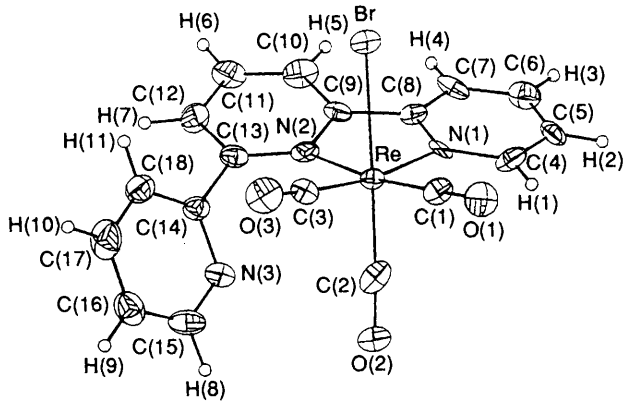

Fig. 6 A view of the X-ray crystal structure of $[ReBr(CO)_3(terpy)]$ showing the atom labelling

Table 5 Energy barriers for restricted rotation of pendant pyridine rings in bidentate metal complexes of terpyridine

Complex	X	Rotamer populations	$\Delta G^{\ddagger}$[a]/kJ mol^{-1}
$[ReX(CO)_3(terpy)]$	Cl	0.55/0.45	36.0 (41.4[b])
	Br	≈0.5/0.5[c]	*d*
	I	0.5/0.5	42.8[b]
$[PtXMe_3(terpy)]$	Cl	0.955/0.045	49.2
	Br	0.924/0.076	50.0
	I	0.867/0.133	48.5

[a] At 298.15 K. [b] At 203 K. [c] Approximate values. [d] Not measurable.

achieved for a rotamer population ratio of 55:45%. The dynamic band shapes were then simulated for different rates of exchange of the two rotamers and some of the 'best-fit' spectra are displayed in Fig. 5. In these simulations full allowance was made for the three-bond *ortho*-hydrogen couplings (*i.e.* J_{HG} = 7.7, J_{LJ} = 7.4 Hz) but longer-range couplings were not included. Satisfactory fittings were achieved over a temperature range −50 to −90 °C from which an activation energy for the rotation was calculated (Table 5).

Low-temperature NMR studies on $[ReI(CO)_3(terpy)]$ revealed similar changes in the composite signal due to the L and H protons. At ambient temperatures this signal consists of two doublets due to three-bond couplings. On cooling the signals broaden, coalesce at *ca.* −70 °C and finally split into an eight-line multiplet which could be simulated quite accurately on the assumption of a 50/50 mixture of two rotameric forms. However, no accurate rotational energy barrier could be computed but a $\Delta G^{\ddagger}$ value based on the coalescence at −70 °C (203 K) was calculated.

Changes in the low-temperature NMR spectra of $[ReBr(CO)_3(terpy)]$ were less pronounced, presumably due to smaller chemical shift differences and no accurate quantitative information on either rotamer populations or rotational energy barriers could be deduced.

In Table 5 the pyridine rotational energy barriers are collected and compared with corresponding values for the $[PtXMe_3(terpy)]$ complexes. In the present rhenium(I) complexes, restriction to rotation of the pendant pyridine ring is clearly substantially less than in the platinum(IV) complexes. This is almost certainly a consequence of the smaller steric interactions of the ring with the less bulky carbonyl ligands as opposed to methyl groups. These interactions must determine the geometries of the preferred solution rotamers and the solid-state structure. The X-ray crystal structure of $[ReBr(CO)_3(terpy)]$ (see later) depicts the pendant pyridine ring at an angle of 52.9° relative to the adjacent co-ordinated ring and with the heterocyclic N atom *trans* to Br. One solution rotamer of the rhenium(I) complexes is therefore attributed to a structure very analogous to the solid-state structure and the other rotamer to the structure where the pyridine ring has rotated by a further 180° so that the heterocyclic N atom has become *cis* to Br. In view of the near equal solution populations of these two rotameric forms their ground-state energies must be extremely similar, and their relative magnitudes could change with halogen. The recently published crystal structure of $[ReCl(CO)_3(terpy)]\cdot H_2O$[10] provides evidence of such a switch-over in relative energies since here the pendant pyridine ring has its N atom *cis* to Cl.

By contrast, in the $PtXMe_3$ complexes of terpyridine,[1] the solution rotamer populations were very dissimilar, the more abundant species varying from 95.5% (for Cl) to 86.7% (for I). In view of the X-ray crystal structure of $[PtIMe_3(terpy)]$, these species are attributed to those with the pendant pyridine N atom *cis* to halogen. As the halogen mass/size decreases from I to Br to Cl, the rotamer equilibrium shifts even further towards the structural form of the solid state as the steric interaction of the heterocyclic N atom with halogen decreases.

Table 6 Fractional atomic coordinates (×10^4) for $[ReBr(CO)_3(terpy)]$

Atom	*x*	*y*	*z*
Re	4049.4(1)	1852.5(4)	8254.4(3)
Br	3596.7(4)	3282.8(13)	9473.6(8)
C(1)	4306(4)	354(12)	9061(8)
O(1)	4477(4)	−551(10)	9552(6)
C(2)	4347(4)	738(12)	7373(9)
O(2)	4513(3)	−30(9)	6855(6)
C(3)	3476(4)	597(12)	8058(8)
O(3)	3121(3)	−158(10)	7983(7)
N(1)	4623(3)	3524(9)	8529(6)
C(4)	5079(4)	3257(13)	8979(7)
C(5)	5413(4)	4394(15)	9196(7)
C(6)	5290(4)	5899(15)	8992(8)
C(7)	4838(5)	6183(13)	8528(8)
C(8)	4512(4)	4982(11)	8304(7)
C(9)	4036(4)	5169(12)	7752(8)
C(10)	3843(5)	6600(12)	7516(8)
C(11)	3411(5)	6705(12)	6977(9)
C(12)	3190(5)	5382(13)	6639(9)
C(13)	3397(4)	3982(12)	6871(7)
N(2)	3806(3)	3873(8)	7465(6)
C(14)	3181(4)	2595(12)	6453(8)
N(3)	3502(4)	1724(11)	6036(7)
C(15)	3310(6)	465(14)	5628(9)
C(16)	2821(6)	96(15)	5576(10)
C(17)	2494(5)	987(18)	5983(11)
C(18)	2680(4)	2274(14)	6430(9)

X-Ray Crystallography.—In order to confirm the bidentate chelate nature of terpyridine in the complexes in the solid state and to compare the structure with other [8–10] bidentate terpyridine complexes, the X-ray crystal structure of $[ReBr(CO)_3(terpy)]$ was determined.

Atomic parameters for the crystal structure of $[ReBr(CO)_3(terpy)]$ are given in Table 6. A view of the molecule indicating the numbering scheme adopted is shown in Fig. 6. This displays the expected *fac* octahedral co-ordination for Re and confirms the bidentate chelate nature of the terpyridine ligand. Bond distances and bond angles are listed in Tables 7 and 8 respectively.

The Re–N distances are unequal with Re–N(2) 2.209 Å and Re–N(1) 2.143 Å. This is also a feature of the three[8–10] published structures involving bidentate terpy and is in contrast to the situation found for terdentate terpyridyl complexes where the metal–nitrogen distance to the central ring is shorter than the corresponding distance to the outer rings.[20]

Inspection of the bond angles at Re (Table 8) shows there to be considerable distortion from a regular octahedral geometry. The main distortions arise from the small bite angle, N(2)–

Table 7 Bond lengths (Å) for [ReBr(CO)$_3$(terpy)]

Br–Re	2.630(4)	C(1)–Re	1.889(13)
C(2)–Re	1.897(15)	C(3)–Re	1.899(13)
N(1)–Re	2.143(10)	N(2)–Re	2.209(10)
O(1)–C(1)	1.157(14)	O(2)–C(2)	1.157(15)
O(3)–C(3)	1.159(14)	C(4)–N(1)	1.371(14)
C(8)–N(1)	1.352(14)	C(5)–C(4)	1.362(16)
C(6)–C(5)	1.391(19)	C(7)–C(6)	1.374(18)
C(8)–C(7)	1.393(15)	C(9)–C(8)	1.478(16)
C(10)–C(9)	1.395(16)	N(2)–C(9)	1.350(13)
C(11)–C(10)	1.363(18)	C(12)–C(11)	1.383(17)
C(13)–C(12)	1.383(16)	N(2)–C(13)	1.363(14)
C(14)–C(13)	1.470(16)	N(3)–C(14)	1.353(15)
C(18)–C(14)	1.375(17)	C(15)–N(3)	1.349(16)
C(16)–C(15)	1.348(20)	C(17)–C(16)	1.367(22)
C(18)–C(17)	1.388(19)		

Table 8 Bond angles (°) for [ReBr(CO)$_3$(terpy)]

C(1)–Re–Br	92.2(5)	C(2)–Re–Br	176.8(3)
C(2)–Re–C(1)	87.0(6)	C(3)–Re–Br	88.1(4)
C(3)–Re–C(1)	86.7(6)	C(3)–Re–C(2)	88.7(6)
N(1)–Re–Br	84.6(3)	N(1)–Re–C(1)	97.8(5)
N(1)–Re–C(2)	98.6(5)	N(1)–Re–C(3)	171.6(4)
N(2)–Re–Br	82.3(3)	N(2)–Re–C(1)	170.7(4)
N(2)–Re–C(2)	98.8(5)	N(2)–Re–C(3)	100.6(5)
N(2)–Re–N(1)	74.3(4)	O(1)–C(1)–Re	178.0(10)
O(2)–C(2)–Re	175.3(9)	O(3)–C(3)–Re	176.5(11)
C(4)–N(1)–Re	125.2(8)	C(8)–N(1)–Re	117.5(8)
C(8)–N(1)–C(4)	117.0(10)	C(5)–C(4)–N(1)	122.4(12)
C(6)–C(5)–C(4)	120.4(12)	C(7)–C(6)–C(5)	117.9(12)
C(8)–C(7)–C(6)	119.7(12)	C(7)–C(8)–N(1)	122.5(11)
C(9)–C(8)–N(1)	114.1(10)	C(9)–C(8)–C(7)	123.3(11)
C(10)–C(9)–C(8)	122.0(11)	N(2)–C(9)–C(8)	116.0(10)
N(2)–C(9)–C(10)	121.9(11)	C(11)–C(10)–C(9)	119.5(11)
C(12)–C(11)–C(10)	118.8(11)	C(13)–C(12)–C(11)	120.2(12)
N(2)–C(13)–C(12)	120.9(11)	C(14)–C(13)–C(12)	119.5(11)
C(14)–C(13)–N(2)	119.5(10)	C(9)–N(2)–Re	113.4(8)
C(13)–N(2)–Re	126.9(7)	C(13)–N(2)–C(9)	118.3(10)
N(3)–C(14)–C(13)	115.3(11)	C(18)–C(14)–C(13)	121.9(11)
C(18)–C(14)–N(3)	122.6(11)	C(15)–N(3)–C(14)	116.4(11)
C(16)–C(15)–N(3)	123.7(13)	C(17)–C(16)–C(15)	120.0(13)
C(18)–C(17)–C(16)	118.1(13)	C(17)–C(18)–C(14)	119.1(13)

Re–N(1) 74.3°, of the terpyridine, and also the angle N(2)–Re–C(3) of 100.6°. This latter value presumably arises because of steric interaction between the unco-ordinated pyridine ring and the carbonyl group C(3)O(3).

The dihedral angles between the ring planes of the terpy and particularly the orientation of the pendant ring are of interest. The two co-ordinated pyridine rings are inclined to each other at an angle of 12° whereas the pendant ring and the adjacent co-ordinated ring are inclined at an angle of 52.9°. The nitrogen atom in the pendant ring is directed towards the axial carbonyl and *trans* to Br. This contrasts with the structure of [ReCl(CO)$_3$(terpy)]·H$_2$O in which the corresponding N atom is *cis* to chlorine.[10]

We are currently extending this work to other metal complexes where terpy is acting as a bidentate chelate ligand, and also studying other N-ligand systems analogous to terpyridine.

Acknowledgements

We are most grateful to the Royal Society for a Visiting Fellowship (for V. S. D.), and to the SERC for a maintenance grant (for H. M. P.).

References

1 Part 1, E. W. Abel, V. S. Dimitrov, N. J. Long, K. G. Orrell, A. G. Osborne, V. Šik, M. B. Hursthouse and M. A. Mazid, *J. Chem. Soc., Dalton Trans.*, 1993, 291.
2 E. C. Constable, *Adv. Inorg. Chem. Radiochem.*, 1987, **30**, 69.
3 N. M. Boag and H. D. Kaesz, *Comprehensive Organometallic Chemistry*, Pergamon, Oxford, 1982, vol. 4, p. 161.
4 M. C. Ganorkar and M. H. B. Stiddard, *J. Chem. Soc.*, 1965, 5346.
5 C. C. Addison, R. Davis and N. Logan, *J. Chem. Soc., Dalton Trans.*, 1974, 2070.
6 R. D. Chapman, R. T. Loda, J. P. Riehl and R. W. Schwartz, *Inorg. Chem.*, 1984, **23**, 1652.
7 A. J. Canty, N. Chaichit, B. M. Gatehouse, E. George and G. Hayhurst, *Inorg. Chem.*, 1981, **20**, 2414.
8 G. B. Deacon, J. M. Patrick, B. W. Skelton, N. C. Thomas and A. H. White, *Aust. J. Chem.*, 1984, **37**, 929.
9 N. C. Thomas and J. Fischer, *J. Coord. Chem.*, 1990, **21**, 119.
10 P. A. Anderson, F. R. Keene, E. Horn and E. R. T. Tiekink, *Appl. Organomet. Chem.*, 1990, **4**, 523.
11 E. W. Abel, N. J. Long, K. G. Orrell, A. G. Osborne, H. M. Pain and V. Šik, *J. Chem. Soc., Chem. Commun.*, 1992, 303.
12 W. Hieber, R. Schuh and H. Fuchs, *Z. Anorg. Allg. Chem.*, 1941, **248**, 243.
13 M. M. Bhatti, Ph.D. Thesis, University of Exeter, 1980.
14 D. F. Shriver, *Manipulation of Air-Sensitive Compounds*, McGraw-Hill, New York, 1969.
15 D. A. Kleier and G. Binsch, DNMR3, Program 165, Quantum Chemistry Program Exchange, Indiana University, IN, 1970.
16 V. Šik, Ph.D. Thesis, University of Exeter, 1979.
17 A. A. Danopoulos, M. B. Hursthouse, B. Hussain-Bates and G. Wilkinson, *J. Chem. Soc., Dalton Trans.*, 1991, 1855.
18 G. M. Sheldrick, SHELX 76, Program for Crystal Structure Determination and Refinement, University of Cambridge, 1976; DIFABS, N. P. C. Walker and D. Stuart, *Acta Crystallogr., Sect. A*, 1983, **39**, 158.
19 K. G. Orrell and V. Šik, *Annu. Rep. NMR Spectrosc.*, 1987, **19**, 155.
20 B. N. Figgis, E. S. Kucharski and A. H. White, *Aust. J. Chem.*, 1983, **36**, 1563.

Received 30*th September* 1992; *Paper* 2/05261J